arXiv:1610.06709v1 [cond-mat.quant-gas] 21 Oct 2016

Stable giant vortex annuli in microwave-coupled atomic condensates

Jieli Qin and Guangjiong Dong

State Key Laboratory of Precision Spectroscopy, Department of Physics, East China Normal University, Shanghai, China
Collaborative Innovation Center of Extreme Optics, Shanxi University, Taiyuan, Shanxi 030006, People's Republic of China

Boris A. Malomed

Department of Physical Electronics, School of Electrical Engineering,
Faculty of Engineering, Tel Aviv University, Ramat Aviv 69978, Israel
Laboratory of Nonlinear-Optical Informatics, ITMO University, St. Petersburg 197101, Russia

Stable self-trapped vortex annuli (VAs) with large values of topological charge S (*giant VAs*) are not only a subject of fundamental interest, but are also sought for various applications, such as quantum information processing and storage. However, in conventional atomic Bose-Einstein condensates (BECs) VAs with $S > 1$ are unstable. Here, we demonstrate that robust self-trapped fundamental solitons (with $S = 0$) and bright VAs (with the stability checked up to $S = 5$), can be created in the free space by means of the local-field effect (the feedback of the BEC on the propagation of electromagnetic waves) in a condensate of two-level atoms coupled by a microwave (MW) field, as well as in a gas of MW-coupled fermions with spin $1/2$. The fundamental solitons and VAs remain stable in the presence of an arbitrarily strong repulsive contact interaction (in that case, the solitons are constructed analytically by means of the Thomas-Fermi approximation). Under the action of the attractive contact interaction with strength β, which, by itself, would lead to collapse, the fundamental solitons and VAs exist and are stable, respectively, at $\beta < \beta_{\max}(S)$ and $\beta < \beta_{\rm st}(S)$, with $\beta_{\rm st}(S = 0) = \beta_{\max}(S = 0)$ and $\beta_{\rm st}(S \geq 1) < \beta_{\max}(S \geq 1)$. Accurate analytical approximations are found for both $\beta_{\rm st}$ and $\beta_{\max}$, with $\beta_{\rm st}(S)$ growing linearly with S. Thus, higher-order VAs are *more robust* than their lower-order couterparts, on the contrary to what is known in other systems that may support stable self-trapped vortices. Conditions for the experimental realizations of the VAs are discussed.

PACS numbers: 03.75.Lm, 05.45.Yv, 42.65.Tg

I. INTRODUCTION

Light and microwaves (MWs) are important tools for controlling dynamics of atomic Bose-Einstein condensates (BECs). In addition to creating traps and optical lattices [1], various optical patterns, including vortices, have potential application in the realm of quantum data processing, as the light patterns can be stored in the form of intrinsic atomic states in BEC, and released back in the optical form [2]. Furthermore, light can generate entangled vortices in separated condensates [3].

The BEC feedback on the light propagation, i.e., the *local field effect* (LFE), may lead to the creation of hybrid light-matter states [4–9]. The electric LFE explains asymmetric matter-wave diffraction [4, 10] and predicts polaritonic solitons in soft optical lattices [5]. Further, the magnetic LFE couples MWs to a pseudo-spinor (two-component) BEC of two-level atoms, thus opening the way to the creation of hybrid microwave-matter-wave solitons [6]. On the other hand, in current experiments with the pseudo-spinor BECs, atoms are first transferred to an intermediate level using a MW field, and then further driven to a target level using a radiation-frequency fields, which would not allow one to observe manifestations of the magnetic LFE. This should become possible if the experiments can be performed with the MW field directly transferring the atoms between the two relevant states.

The LFE plays an increasingly important role in BEC with the increase of the number of atoms, which can exceed 10^8, as predicted theoretically [11] and demonstrated experimentally [12], allowing the LFE-induced long-range interactions between atoms [5, 6] to produce new manifestations of nonlocal physics. Actually, the long-range interaction may cover the whole gas, in contrast with fast-decaying nonlocal interactions in optics [13] and in dipolar BEC [14–19]. Unlike the species-dependent dipolar forces [14–17], the LFE-induced interaction can be realized in any ultracold atomic or molecular gas [6].

The LFE was not previously explored in two- and three-dimensional (2D and 3D) settings, where it may give rise to new phenomenology in comparison with the recently investigated 1D case [4–6], as the LFE-induced interaction is determined by the underlying Green's function, which has different forms in effectively 1D, 2D, and 3D geometries (note that the above-mentioned "massive" BEC, with a large number of atoms $\gtrsim 10^8$, can be readily morphed into a low-dimensional shape [12]). In particular, we demonstrate here that solitary vortices, alias vortex annuli (VAs), readily self-trap in the 2D setting. Vortices in BEC are essential for simulating various effects from condensed matter [20], and as building blocks of quantum turbulence [21]. They also help to emulate gravitational physics [22], and find applications, such as phase qubits [23] and matter-wave Sagnac interferometers for testing the rotational-equivalence principle [25, 26]. As mentioned above, atomic-matter vortices can store and release information delivered by optical vortex beams [2].

The stabilization of VAs with large values of the topolog-

ical charge (vorticity) S, which is required for deterministic creation of vortices [28] and for applications (in particular, the storage of higher-order optical vortices in the form of their atomic counterparts), is a challenging issue [27]. Under repulsive interactions, vortices supported by a nonzero background are stable solely for $S=1$, while vortices with $S\geq 2$ split into ones with $S=1$ [27]. For the above-mentioned applications, most relevant are bright VAs in BEC with attractive nonlinearity. Unlike nonlinear optics, where VAs can be stabilized by non-Kerr nonlinearities [29], in BEC with attractive interactions the only setting which gives rise to stable 2D [30] and 3D [31] *semi-vortices* (with $S_\uparrow=1$ and $S_\downarrow=0$ in their two components) in the free space is provided by the spin-orbit coupling. However, all higher-order states, with $S_\uparrow=1+s$, $S_\downarrow=s\geq 1$, are unstable. The family of single-component modes with $S=1$ may be partly stabilized by a trapping potential, but all the higher-order VAs with $S\geq 2$ remain unstable in this case too [32]. Partly stable VAs with $S\geq 2$ were predicted only in "exotic" settings, with the local strength of the repulsive nonlinearity in the space of dimension D growing with distance r from the center faster than r^D [33], or making use of a combination of a trapping potential and a *spatially localized* attractive interaction [34].

In this work, we introduce a 2D hybrid system consisting of a pseudo-spinor BEC whose two components are coupled by a MW field through a magnetic-dipole transition. The system gives rise to *stable* giant VAs, i.e., ones with *arbitrarily high* values of S (the stability checked up to $S=5$). This is as well possible in the presence of additional contact repulsive interactions. On the other hand, under the action of an attractive contact interaction, with strength β, which drives the critical collapse in the 2D geometry [35], the VAs exist and are stable, respectively, for $\beta<\beta_{\max}$ and $\beta<\beta_{\rm st}\leq\beta_{\max}$. We demonstrate, by means of analytical and numerical considerations, that $\beta_{\rm st}$ linearly grows with S, thus making higher-order vortices *more robust* than lower-order ones, opposite to what is known in few other models capable to support stable higher-order VAs [33, 34]. It is relevant to mention that the concept of giant vortices is known in the usual BEC settings with the contact repulsion [36], where they are not self-trapped objects, i.e., they are not VAs.

The rest of the paper is organized as follows. The model is introduced in Section II, numerical and analytical results are collected in Section III, and the paper is concluded by Section IV.

II. THE MODEL

As schematically shown in Fig. 1, we consider a nearly-2D (pancake-shaped) binary BEC composed of two different hyperfine states of the same atomic species, which is described by the two-component (pseudo-spinor) wave function, $|\Psi\rangle=\left(\Psi_\downarrow,\Psi_\uparrow\right)^T$, with each component emulating "spin-up" and "spin-down" states. The corresponding Hamiltonian is $\mathcal{H}=\hat{\mathbf{p}}^2/2m_{\rm at}-(\hbar\delta/2)\sigma_3-\mathbf{m}\cdot\mathbf{B}$ [6], where $m_{\rm at}$, $\hat{\mathbf{p}}$, and $\mathbf{m}$ are the atomic mass, 2D momentum, and magnetic moment, $\hbar\delta$ an energy difference between atomic states $|\uparrow\rangle$ and $|\downarrow\rangle$, σ_3

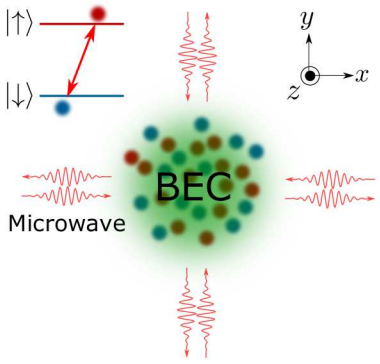

FIG. 1: Two hyperfine atomic states coupled by the MW (microwave) field in a pancake-shaped BEC. The MW field is polarized in the direction perpendicular to the pancake's plane.

the Pauli matrix, and $\mathbf{B}=\mu_0(\mathbf{H}+\mathbf{M})$ is the magnetic induction, with magnetic field $\mathbf{H}$ and magnetization $\mathbf{M}=\langle\Psi|\,\mathbf{m}\,|\Psi\rangle$. In the rotating-wave approximation, the atomic wave function, $|\psi\rangle\equiv|\phi\rangle\,e^{\pm i\omega t/2}\equiv\left(\phi_\downarrow,\phi_\uparrow\right)^T$, is governed by coupled Gross-Pitaevskii equations (GPEs), with $*$ standing for the complex conjugate:

$$\begin{aligned} i\hbar\partial\phi_\downarrow/\partial t &= \left(\hat{\mathbf{p}}^2/2m_{\rm at}+\hbar\Delta/2-\mu_0\mathbf{m}_{\uparrow\downarrow}\cdot\mathbf{m}_{\downarrow\uparrow}\left|\phi_\uparrow\right|^2\right)\phi_\downarrow \\ &\quad -\mu_0\mathbf{m}_{\downarrow\uparrow}\cdot\mathbf{H}^*\phi_\uparrow, \\ i\hbar\partial\phi_\uparrow/\partial t &= \left(\hat{\mathbf{p}}^2/2m_{\rm at}-\hbar\Delta/2-\mu_0\mathbf{m}_{\uparrow\downarrow}\cdot\mathbf{m}_{\downarrow\uparrow}\left|\phi_\downarrow\right|^2\right)\phi_\uparrow \\ &\quad -\mu_0\mathbf{m}_{\uparrow\downarrow}\cdot\mathbf{H}\phi_\downarrow, \end{aligned} \tag{1}$$

with detuning $\Delta=\omega-\delta$ of the MW from the atomic transition, and matrix elements of the magnetic moment, $\mathbf{m}_{\uparrow\downarrow}$ and $\mathbf{m}_{\downarrow\uparrow}$ ($\mathbf{m}_{\uparrow\uparrow}=\mathbf{m}_{\downarrow\downarrow}=0$ due to the symmetry).

The magnetic field and magnetization, which are polarized perpendicular to the pancake's plane, are each represented by a single component, H and M, which obey the Helmholtz equation,

$$\nabla^2H+k^2H=-k^2M, \tag{2}$$

where k is the MW wavenumber. As the wavelength of the MW field, $\lambda=2\pi/k$, is always much greater than an experimentally relevant size of the BEC, the second term in Eq. (2) may be omitted in comparison with the first term (see also Ref. [6]), reducing Eq. (2) to the Poisson equation for the scalar field:

$$\nabla^2H=-k^2M. \tag{3}$$

Because the medium's magnetization, which is the source of the magnetic field, is concentrated in the pancake, the Poisson equation may be treated as one in the 2D plane. Them using the Green's function of the 2D Poisson equation, the magnetic field is given by

$$H=H_0-Nk^2\left|\mathbf{m}_{\downarrow\uparrow}\right|/(2\pi l_\perp)\int\ln\left(\left|\mathbf{r}-\mathbf{r}'\right|\right)\phi_\downarrow^*\left(\mathbf{r}'\right)\phi_\uparrow\left(\mathbf{r}'\right)d\mathbf{r}', \tag{4}$$

where H_0 is a background magnetic field of the MW, N is the number of atoms, and $\mathbf{r}$ is the set of 2D coordinates normalized by the transverse confinement size $l_\perp$. Then, the GPEs for the wave function, subject to normalization $\int\left(|\phi_\uparrow|^2+|\phi_\downarrow|^2\right)d\mathbf{r}=1$, takes the form of

$$i\frac{\partial\phi_\downarrow}{\partial\tau}=\left(-\frac{1}{2}\nabla^2+\eta+H_0-\beta|\phi_\uparrow|^2\right)\phi_\downarrow +\frac{\gamma\phi_\uparrow}{2\pi}\int\ln\left(|\mathbf{r}-\mathbf{r}'|\right)\phi_\downarrow(\mathbf{r}')\,\phi_\uparrow^*(\mathbf{r}')\,d\mathbf{r}', \tag{5}$$

$$i\frac{\partial\phi_\uparrow}{\partial\tau}=\left(-\frac{1}{2}\nabla^2-\eta+H_0-\beta|\phi_\downarrow|^2\right)\phi_\uparrow +\frac{\gamma\phi_\downarrow}{2\pi}\int\ln\left(|\mathbf{r}-\mathbf{r}'|\right)\phi_\downarrow^*(\mathbf{r}')\,\phi_\uparrow(\mathbf{r}')\,d\mathbf{r}', \tag{6}$$

where rescaling is defined by $\phi_{\uparrow,\downarrow}=\sqrt{N}/l_\perp\psi_{\uparrow,\downarrow}$, $\tau=t/t_0$ with $t_0=\hbar/E_c$ and $E_c=\hbar^2/(m_{\rm at}l_\perp^2)$, $\eta\equiv t_0\Delta/2$, and scaled strengths of the LFE and contact interactions (if any) are

$$\gamma=m_{\rm at}l_\perp k^2N\mu_0|\mathbf{m}_\uparrow|^2/\hbar^2,\ \beta\equiv N\mu_0\mathbf{m}_{\uparrow\downarrow}\cdot\mathbf{m}_{\downarrow\uparrow}/\left(\hbar l_\perp^3E_c\right). \tag{7}$$

To describe experimental conditions, three-dimensional should also include the trapping potential, $\left(\Omega^2/2\right)r^2\phi_{\uparrow,\downarrow}$. It has been checked that, after the creation of the trapped modes, the potential may be switched off, leading to smooth transformation of the modes into their self-trapped counterparts obtained directly found in the free space ($\Omega=0$). The vorticity may be imparted to the trapped condensate by a vortical optical beam [2].

If collisions between atoms belonging to the two components are considered (with the corresponding strength of the contact interaction tunable by dint of the Feshbach resonance [37]), the additional cross-cubic terms can be absorbed into rescaled coefficient β. Collisions may also give rise to self-interaction terms, $-\tilde{\beta}|\phi_\downarrow|^2$ and $\tilde{\beta}|\phi_\uparrow|^2$, in the parentheses of Eqs. (5) and (6), respectively. On the other hand, the same equations with $\beta=0$ apply as well to a different physical setting, *viz.*, a degenerate Fermi gas with spin $1/2$, in which $\phi_\downarrow$ and $\phi_\uparrow$ represent two spin components, coupled by the MW magnetic field [6, 38].

The following analysis is chiefly dealing with the zero-detuning (symmetric) system, $\eta=0$. In this case, Eqs. (5) and (6) coalesce into a single equation for $\phi_\downarrow=\phi_\uparrow\equiv\phi\exp\left(-iH_0\tau\right)$, subject to normalization $\int|\phi(\mathbf{r})|^2d\mathbf{r}=1/2$:

$$i\frac{\partial\phi}{\partial\tau}=\left[-\frac{1}{2}\nabla^2-\beta|\phi|^2+\frac{\gamma}{2\pi}\int\ln\left(|\mathbf{r}-\mathbf{r}'|\right)|\phi(\mathbf{r}')|^2d\mathbf{r}'\right]\phi, \tag{8}$$

and the above-mentioned self-interaction coefficient, $\tilde{\beta}$, may be absorbed into β. This equation and the normalization condition are invariant with respect to the self-similarity transformation: $\phi(\mathbf{r},\tau)=\sqrt{\gamma_0}\tilde{\phi}(\tilde{\mathbf{r}},\tau)\exp\left\{-i\left[\gamma(\ln\gamma_0)/8\pi\right]\tau\right\}$, $\tau=\gamma_0^{-1}\tilde{\tau}$, $\mathbf{r}=\gamma_0^{-1/2}\tilde{\mathbf{r}}$, $\gamma=\gamma_0\tilde{\gamma}$, $\beta\equiv\tilde{\beta}$, which allows one to replace γ by γ/γ_0 with arbitrary factor γ_0. We use this option to to fix $\gamma=\pi$ in the numerical analysis of the symmetric configuration. In physical units, for alkali atoms transversely confined with $l_\perp=1$ μm and irradiated by a MW with wavelength 1 mm, the above definition yields $\gamma\sim10^{-7}N$. Thus, $\gamma\sim10$ for the experimentally available "massive" BEC with $N\sim10^8$ [11, 12], while a typical VA radius can be estimated as ~10 μm (see Figs. 2 and 5 below), and a characteristic range of the magnetic-field amplitudes may reach a few gauss.

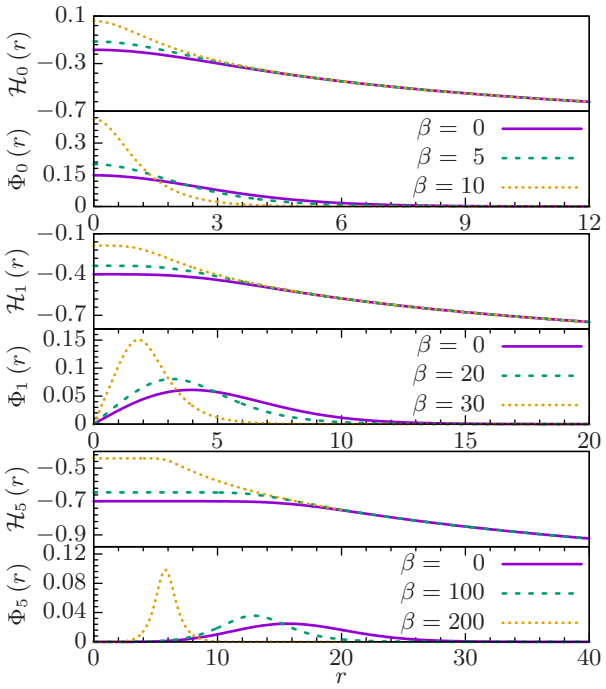

FIG. 2: Radial profiles of the magnetic filed and wave functions in fundamental solitons (top) and vortices with $S=1$ (middle) and $S=5$ (bottom) at indicated values of β.

III. THE RESULTS

Stationary solutions to Eq. (8) with chemical potential μ and vorticity S are looked for, in polar coordinates (r,θ), as

$$\phi=e^{-i\mu\tau-iS\theta}\Phi_S(r), \tag{9}$$

where $\Phi_S(r)$ is a real radial wave function. Typical examples of solutions for $\Phi_S(r)$, produced by the imaginary-time evolution method [39], are plotted in Fig. (2), for different values of S and $\beta\geq0$. Numerical results demonstrate that fundamental solitons (which correspond to $S=0$) and VAs are destroyed by the collapse at $\beta>\beta_{\rm max}(S)$, see Table I. This critical value can be found by considering the energy corresponding to Eqs. (5) and (6) with $\phi_\uparrow=\phi_\downarrow$,

$$E=2\pi\int_0^\infty rdr\left[(\Phi_S')^2+r^{-2}S^2\Phi_S^2-\beta\Phi_S^4\right] +\frac{\gamma}{2\pi}\int\int d\mathbf{r}_1d\mathbf{r}_2\ln\left(|\mathbf{r}_1-\mathbf{r}_2|\right)\Phi_S^2(\mathbf{r}_1)\Phi_S^2(\mathbf{r}_2). \tag{10}$$

The numerical findings displayed in Figs. 2 and 5 suggest that, for $S\geq2$ and β large enough, the vortex takes the shape

S	$\beta_{\max}$	$\beta_{\max}^{(\mathrm{an})}$	β_{st}	S	$\beta_{\max}$	$\beta_{\max}^{(\mathrm{an})}$	β_{st}
0	11.8	n/a	$\equiv\beta_{\max}$	3	132.5	130.6	41
1	48.3	43.5	11	4	175.5	174.1	57
2	89.7	87.0	28	5	218.5	217.7	70

TABLE I: $\beta_{\max}$ and $\beta_{\max}^{(\mathrm{an})}$: numerically obtained and analytically predicted values of the contact-interaction strength, β, up to which the fundamental solitons and vortex annuli exist. β_{st}: the numerically identified stability boundary of the vortex annuli.

of a narrow annulus, which may be approximated by the usual quasi-1D soliton shape in the radial direction, with regard to the adopted normalization, cf. Ref. [49]:

$$\Phi_S(r) = \sqrt{\beta}/\left(8\pi R\right)\mathrm{sech}[\beta\left(r-R\right)/\left(8\pi R\right)], \tag{11}$$

where R is the VA's radius. The substitution of this approximation in Eq. (10) yields

$$E(R) = \left[S^2 - \frac{\beta^2}{3\left(8\pi\right)^2}\right]\frac{1}{2R^2} + \frac{\gamma}{8\pi}\ln R. \tag{12}$$

Next, the annulus' radius R is to be selected as a point corresponding to the energy minimum: $dE/dR = 0$, i.e., $R_{\min}^2 = \left(8\pi/\gamma\right)\left[S^2 - \left(1/3\right)\left(\beta/8\pi\right)^2\right]$ (comparison with numerical results demonstrates that $R_{\min}$ provides a reasonable approximation for the radius of narrow VAs). Then, $\beta_{\max}$ is predicted as the value at which $R_{\min}^2$ vanishes, i.e., the annulus collapses to the center,

$$\beta_{\max}^{(\mathrm{an})} = 8\sqrt{3}\pi S. \tag{13}$$

As seen in Table I, this analytical prediction is virtually identical to its numerically found counterparts at $S \geq 2$.

Further, it is found that $\beta_{\max}$ is the same as in the "simplified" 2D GPE that contains solely the local-attraction term,

$$i\partial\phi/\partial\tau = -\left[\left(1/2\right)\nabla^2 + \beta\left|\phi\right|^2\right]\phi, \tag{14}$$

for which the existence limit was found in Refs. [41], for $S = 0$, and in Ref. [40] for $1 \leq S \leq 5$, i.e., $\beta_{\max}$ does not depend of the LFE strength, γ. To explain this fact, we note that, at the limit stage of the collapse, when the shrinking 2D annulus becomes extremely narrow, the equation for the wave function becomes asymptotically tantamount to Eq. (14), therefore the condition for the onset of the collapse is identical in both equations. However, the solitons of Eq. (14) exist solely at $\beta = \beta_{\max}$, being completely unstable, while the LFE-induced long-range interaction in Eqs. (5) and (6) creates *stable* solitons and vortices for all S, as shown below. It is worthy to stress too that the analytical result given by Eq. (13) provides an explanation for the numerical findings that were first reported in Ref. [40] and later considered in many works, but never reproduced in an analytical form.

The stability of the self-trapped modes has been systematically tested by real-time simulations of Eqs. (5) and (6)

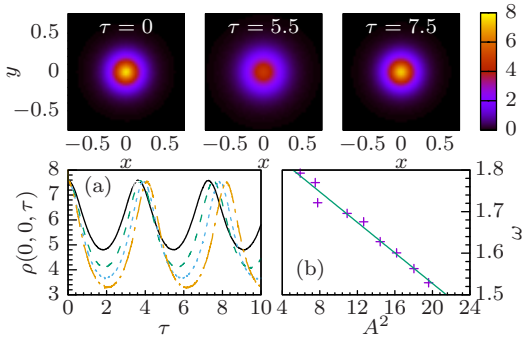

FIG. 3: (a) Oscillations of the peak density, $\rho\left(0,0\right) \equiv \left|\phi_{\downarrow}(x=y=0)\right|^2 + \left|\phi_{\uparrow}(x=y=0)\right|^2$, of the perturbed fundamental soliton at $\beta = 11.6$ (for different perturbation amplitudes). (b) The oscillation frequency vs. the squared oscillation amplitude, A^2. The top row displays profiles of the oscillating soliton.

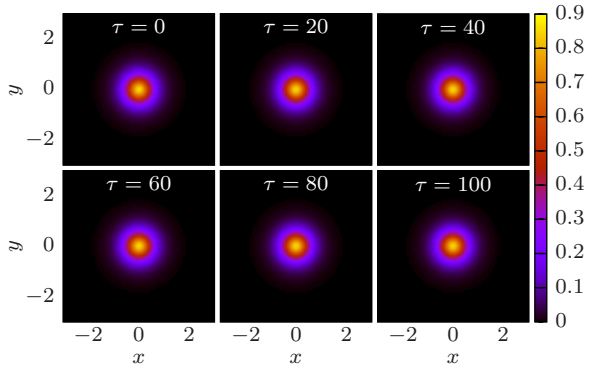

FIG. 4: Stable perturbed evolution of the fundamental soliton, with $S = 0$ and $\beta = 11$. Note that this value of β is close to the existence boundary, $\beta_{\max}(S=0) = 11.8$, see Table 1.

with random perturbations added to the stationary solutions (independent perturbations were taken for $\phi_{\uparrow}$ and $\phi_{\uparrow}$, to verify the stability against breaking the symmetry between them). The fundamental solitons are stable in their entire existence region, $\beta < \beta_{\max} \approx 11.8$. At β very close to $\beta_{\max}$, the perturbations lead to persistent oscillations, as shown in Fig. 3(a) for $\beta = 11.6$, due to excitation of a soliton's internal mode [43–45]. It is seen in Fig. 3(b) that the oscillation frequency is a nearly linear function of the squared amplitude of the oscillations, which is a typical feature of a nonlinear oscillatory mode.

Systematic simulations of the evolution of the VA families reveal an internal stability boundary, $\beta_{\mathrm{st}}(S) < \beta_{\max}(S)$ (see Table 1), the vortices being stable at $\beta < \beta_{\mathrm{st}}(S)$. In the interval of $\beta_{\mathrm{st}}(S) < \beta < \beta_{\max}(0)$, they are broken by azimuthal perturbations into rotating necklace-shaped sets of fragments, which resembles the initial stage of the instability development of localized vortices in usual models [29, 32, 46, 47]; however, unlike those models, the necklace does not expand, remaining confined under the action of the effective nonlocal interaction. Typical examples of the stable and unstable evolution of fundamental solitons and VAs are displayed, respectively, in Figs. 4 and 5.

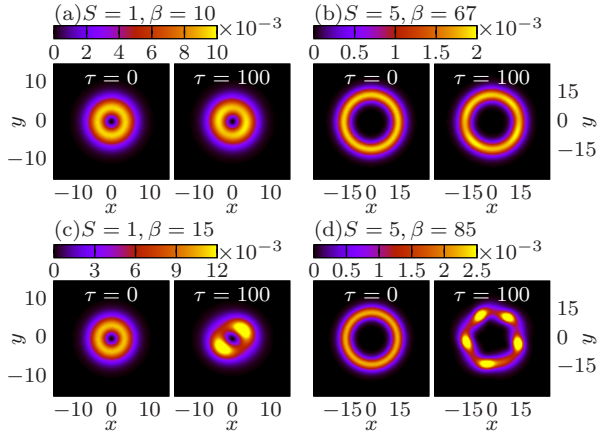

FIG. 5: Top and bottom panels display, severally, examples of the stable and unstable perturbed evolution of the VAs with indicated values of S and β. The necklace-shaped set, observed in the latter case, remains confined (keeping the same overall radius) in the course of subsequent evolution.

To address the stability of the VAs against azimuthal perturbations in an analytical form, we approximate the wave function of a perturbed VA by $A(\theta)\Phi_S(r)$ and derive an evolution equation for the modulation amplitude, A, by averaging Eqs. (5)-(6) in the radial direction:

$$i\frac{\partial A}{\partial\tau}=-\frac{1}{2R^2}\frac{\partial^2 A}{\partial\theta^2}+\left[\frac{\gamma\ln R}{4\pi R}-\frac{2\beta^2}{3\left(8\pi R\right)^2}\right]|A|^2A. \qquad (15)$$

A straightforward analysis of the modulational stability of the solution with $A=1$ against perturbations $\sim\exp\left(ip\theta\right)$ with integer winding numbers p [50] shows that the stability is maintained under the threshold condition, $p^2\geq(8/3)\left(\beta/8\pi\right)^2$, if the term $\sim\beta^2$ dominates in Eq. (15). Further, the numerical results demonstrate that, as in other models [51], the critical instability corresponds to $p^2=S^2$ (for instance, the appearance of five fragments in the part of Fig. 5 corresponding to $S=5,\beta=85$ demonstrates that, for $S=5$, the dominant splitting mode has $p=5$). Thus, it is expected that the VAs remain stable at $\beta<\beta_{\rm st}^{\rm (an)}(S)=2\sqrt{6}\pi S\approx15.4S$. On the other hand, the numerically found stability limits collected in Table 1 obey an empirical formula, $\beta_{\rm st}^{\rm (num)}(S)\approx15S-4$. Thus, the analytical approximation is quite accurate for $S\geq2$. To put this result in a physical context, we note that, in terms of experimentally relevant parameters, the scaling adopted above implies $|\beta|\sim\left(|a_s|/l_\perp\right)N$, where $a_s<0$ is the scattering length which accounts for the contact attraction. Thus, values of β (actually, of either sign) may be relevant up to $|\beta|\sim1000$.

It follows from these results that the giant VAs, with higher values of S, are *much more robust* than their counterparts with smaller S. This feature is opposite to what was previously found in those (few) models which are able to produce stable VAs with $S>1$ [29, 33, 34]. It is relevant to mention that, at $\beta<\beta_{\rm st}(S=0)$, the fundamental soliton is the system's ground state, while, at $\beta>\beta_{\rm st}(S=0)$, the ground state does not exist, due to the possibility of the collapse. The vortices with $\beta_{\rm st}(S)>\beta$ cannot represent the ground state, but,

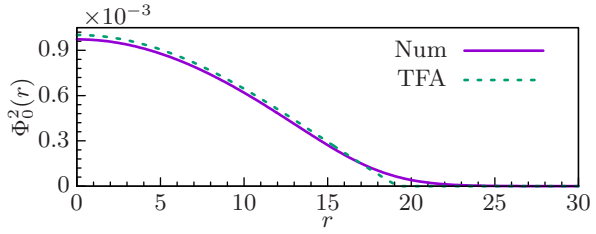

FIG. 6: Comparison of the Thomas-Fermi approximation, as given by Eq. (16), for the fundamental soliton (the dashed line) and its numerically found counterpart (the solid line), for $\beta=-200$.

nevertheless, they exist as metastable ones, cf. the spin-orbit-coupled system, considered in Ref. [31], where self-trapped three-dimensional modes of the semi-vortex type exist too as metastable states, although the system does not have a ground state, due to the presence of the supercritical collapse.

For the strong *repulsive* contact interaction (large $\beta<0$), fundamental solitons (with $S=0$) can be constructed by means of the Thomas-Fermi approximation (TFA), as shown by straightforward consideration of the stationary version of Eq. (8), with the substitution of the stationary wave form as per Eq. (9). In this case, it is more convenient, instead of using the Green's function, to explicitly combine the stationary equation with Poisson equation (3). The result is

$$\left(\Phi_0^2\right)_{\rm TFA}(r)=\begin{cases}\phi_0^2J_0\left(\xi r\right) \ \text{ at } \ r<r_1/\xi,\\ \left(\Phi_0^2\right)_{\rm TFA}(r)=0 \ \text{ at } \ r>r_1/\xi\,,\end{cases} \qquad (16)$$

where $\xi\equiv\sqrt{\gamma/|\beta|}$, $r_1\approx2.4$ is the first zero of Bessel function $J_0(r)$, and ϕ_0 is a normalization constant. Figure 6 shows that the TFA agrees very well with the numerical solution.

Lastly, it is relevant to proceed from the symmetric system [$\eta=0$, $\phi_\uparrow=\phi_\downarrow$ in Eqs. (5) and (6)] to a strongly asymmetric one, with large η. The relevant solution has $\mu=-\eta+\delta\mu$ with $|\delta\mu|\ll\eta$ and small component $\Phi_\downarrow\approx\left(H_0/2\eta\right)\Phi_\uparrow$, while the large one satisfies equation

$$\left(\Delta\mu+\frac{H_0^2}{2\eta}\right)\Phi_\uparrow=-\tfrac{1}{2}\nabla^2\Phi_\uparrow-\tfrac{\beta H_0^2}{4\eta^2}\Phi_\uparrow^3-\tfrac{\gamma H_0^2}{8\pi\eta^2}\Phi_\uparrow \int\ln\left(|\mathbf{r}-\mathbf{r}'|\right)\Phi_\uparrow^2(\mathbf{r}')d\mathbf{r}'. \qquad (17)$$

Up to obvious rescaling, Eq. (17) is identical to the equation for the stationary wave function in the symmetric case, i.e., Eq. (8) with substitution of the wave function as per Eq. (9), with any value of S. Thus, the strongly asymmetric solutions can obtained by means of the rescaling of their symmetric counterparts.

IV. CONCLUSION

In this work we have developed the analysis for the 2D fundamental solitons and VAs (vortex annuli) produced by the LFE (local field effect) in the BEC composed of two-level atoms, or, alternatively, a gas of fermions, in which two components are coupled by the MW (microwave) field. The effective long-range interaction mediated by the field stabilizes

the solitons and VAs, even in the presence of the attractive contact interaction between the two components, which, by itself, leads to the critical collapse. The solitons exists too and are stable in the presence of the arbitrarily strong contact repulsion. Nearly exact critical values of the local-attraction strength, $\beta_{\max}$, up to which the solitons and vortices exist, have been found analytically. This result also provides an analytical explanation to the well-known existence limits of VAs in the 2D nonlinear Schrödinger/Gross-Pitaevskii equation with the cubic self-focusing term, which were previously known solely in the numerical form. While the fundamental solitons are stable up to $\beta = \beta_{\max}$, the VAs remain stable in a smaller interval, $\beta \leq \beta_{\rm st} < \beta_{\max}$, being vulnerable to the azimuthal instability at $\beta_{\rm st} < \beta < \beta_{\max}$. The stability boundary, $\beta_{\rm st}$, is found in an approximate analytical form too. On the contrary to previously studied models [29, 33, 34], the (giant) VAs with higher vorticities, such as $S = 5$, are more robust than their counterparts with small S. In addition, a very accurate TFA (Thomas-Fermi approximation) was developed for the fundamental solitons, with $S = 0$. The results have been obtained for both symmetric and strongly asymmetric two-component systems.

The VAs obtained here can be further used to construct vortex lattices [48]. Challenging possibilities are to consider interaction between the self-trapped modes, and, eventually, to extend the model to the fully 3D setting. Another direction for the extension of the work is to explore the electric LFE in a molecular condensate.

Acknowledgments

This work was supported, in part, by National Science Foundation of China (grants Nos. 11574085 and 91536218), the Research Fund for the Doctoral Program of Higher Education of China (grant No. 20120076110010), Program of Introducing Talents of Discipline to Universities (B12024), and by the joint program in physics between the National Science Foundation (US) and Binational Science Foundation (US-Israel), through grant No. 2015616. B.A.M. appreciates hospitality of the State Key Laboratory of Precision Spectroscopy and Department of Physics at the East China Normal University.

[1] C. S. Adams, M. Sigel, and J. Mlynek, Phys. Rep. **240**, 143(1994); G. Grynberg and C. Robilliard, *ibid*. **355**, 335(2001); V. A. Brazhnyi and V. V. Konotop, Mod. Phys. Lett. B **18**, 627 (2004); O. Morsch and M. Oberthaler, Rev. Mod. Phys. **78**, 179 (2006); I. Bloch, J. Dalibard, and W. Zwerger, *ibid*. **80**, 885 (2008); S. Giorgini, L. P. Pitaevskii, and S. Stringari, *ibid*. **80**, 1215 (2008).

[2] M. F. Andersen, C. Ryu, P. Cladé, V. Natarajan, A. Vaziri, K. Helmerson, and W. D. Phillips, Phys. Rev. Lett. **97**, 170406 (2006); R. Pugatch, M. Shuker, O. Firstenberg, A. Ron, and N. Davidson, *ibid*. **98**, 203601 (2007); M. Shuker, O. Firstenberg, R. Pugatch, A. Ron, and N. Davidson, *ibid*. **100**, 223601 (2008).

[3] N. Lo Gullo, S. McEndoo, T. Busch, and M. Paternostro, Phys. Rev. A **81**, 053625 (2010).

[4] J. Zhu, G. J. Dong, M. N. Shneider, and W. Zhang, Phys. Rev. Lett. **106**, 210403 (2011).

[5] G. J. Dong, J. Zhu, W. Zhang, and B. A. Malomed, Phys. Rev. Lett. **110**, 250401 (2013).

[6] J. L. Qin, G. J. Dong, and B. A. Malomed, Phys. Rev. Lett. **115**, 023901 (2015).

[7] F. Cattani, A. Kim, M. Lisak, and D. Anderson, Int. J. Mod. Phys. B **27**, 1330003(2013).

[8] G. Labeyrie, E. Tesio, P. M. Gomes, G.-L. Oppo, W. J. Firth, G. R. M. Robb, A. S. Arnold, R. Kaiser, and T. Ackemann, Nature Phot. **8**, 321 (2014).

[9] T. J. Mendonca and R. Kaiser, Phys. Rev. Lett. **108**, 033001 (2012).

[10] K. Li, L. Deng, E. W. Hagley, M. G. Payne, and M. S. Zhan, Phys. Rev. Lett. **101**, 250401 (2008).

[11] D. Comparat, A. Fioretti, G. Stern, E. Dimova, B. Laburthe Tolra, and P. Pillet, Phys. Rev. A **73**, 043410 (2006).

[12] K. M. van der Stam, E. D. van Ooijen, R. Meppelink, J. M. Vogels, and P. van der Straten, Rev. Sci. Instrum. **78**, 013102 (2007); H. Imai, T. Akatsuka, T. Ode, and A. Morinaga, Phys. Rev. A **85**, 013633 (2012).

[13] R. Barboza, U. Bortolozzo,M. G. Clerc, S. Residori, and E. Vidal-Henriquez, Adv. Opt. Phot. **7**, 635 (2015).

[14] A. Griesmaier, J. Werner, S. Hensler, J. Stuhler and T. Pfau, Phys. Rev. Lett. **94**, 160401 (2005)

[15] M. Lu, N. Q. Burdick, S. H. Youn, and B. L. Lev, Phys. Rev. Lett. **107**, 190401 (2011); M. Lu, N. Q. Burdick, and B. L. Lev, *ibid.* **108** 215301 (2012)

[16] K. Aikawa, A. Frisch, M. Mark, S. Baier,A. Rietzler, R. Grimm and F. Ferlaino , *ibid.* 108 210401 (2012), K. Aikawa,A. Frisch, M. Mark,A. Baier, R. Grimm and F. Ferlaino, *ibid.* **112**, 010404 (2014).

[17] K. - K. Ni, S. Ospelkaus, M. H. G. de Miranda, A. Pe'er, B. Neyenhuis, J. J. Zirbel, S. Kotochigova, P. S. Julienne, D. S. Jin, and J. Ye, Science **322**, 231 (2008); J. Deiglmayr, A. Grochola, M. Repp, K. Mötlbauer, C. Glük, J. Lange, O. Dulieu, R. Wester, and M. Weidemüler, Phys. Rev. Lett. **101**, 133004 (2008).

[18] P. Pedri and L. Santos, Phys. Rev. Lett. **95**, 200404 (2005); F. Maucher, N. Henkel, M. Saffman, W. Krolikowski, S. Skupin and T. Pohl, *ibid* **106**, 170401 (2011); F. Maucher, S. Skupin, M. Shen, and W. Królikowski, Phys. Rev. A **81**, 063617 (2010).

[19] T. Lahaye, C. Menotti, L. Santos, M. Lewenstein, and T. Pfau, Rep. Prog. Phys. **72**, 126401 (2009).

[20] T. P. Simula and P. B. Blakie, Phys. Rev. Lett. **96**, 020404 (2006); Z. Hadzibabic, P. Krüger, M. Cheneau, B. Battelier, and J. Dalibard, Nature 441, 1118 (2006); M. J. Davis, S. A. Morgan, and K. Burnett, Phys. Rev. Lett. **66**, 053618 (2002); N. G. Berloff and B. V. Svistunov, Phys. Rev. A **66**, 013603 (2002);S.-W. Su, S.-C. Gou, A. Bradley, O. Fialko, and J. Brand, Phys. Rev. Lett. **110**, 215302(2013);Paul M. Chesler, Antonio M. Garcí-Garcí, and Hong Liu,Phys. Rev. X **5**, 021015 (2015)

[21] V. I. Yukalov, A. N. Novikov, and V. S. Bagnato, J. Low Temp. Phys. **180**, 53 (2015); E. A. L. Henn, J. A. Seman, G. Roati, K. M. F. Magalhães, and V. S. Bagnato, Phys. Rev. Lett. **103**, 045301 (2009). E. A. L. Henn, J. A. Seman, G. Roati, K. M.

F. Magalhães, and V. S. Bagnato, Journal of Low Temperature Physics **158**, 435 (2009); T. W. Neely, A. S. Bradley, E. C. Samson, S. J. Rooney, E. M. Wright, K. J. H. Law, R. Carretero-González, P. G. Kevrekidis, M. J. Davis, and B. P. Anderson, Phys. Rev. Lett. 111, 235301 (2013);T. Simula, M. J. Davis, and K. Helmerson, Phys. Rev. Lett. **113**, 165302 (2014); W. J. Kwon, G. Moon, J. Y. Choi, S. W. Seo, and Y.-i. Shin, Phys. Rev. A **90**, 063627 (2014). W. J. Kwon, G. Moon, S. W. Seo, and Y. Shin, Phys. Rev. A **91**, 053615 (2015); G. W. Stagg, A. J. Allen, N. G. Parker, and C. F. Barenghi, Phys. Rev. A **91**, 013612 (2015)

[22] N. G. Parker, B. Jackson, A. M. Martin, and C. S. Adams,*Vortices in Bose-Einstein Condensates: Theory, Emergent Nonlinear Phenomena in Bose-Einstein Condensates* (Springer, 2008); N. T. Zinner, Phys. Res. Int. 2011, 734543 (2011); F. Federici, C. Cherubini, S. Succi, and M.P. Tosi, Phys. Rev. A **73**, 033604 (2006); F. Künel and C. Rampf, Phys. Rev. D **90**, 103526 (2014); T. Harko, Phys. Rev. D **89**, 084040 (2014).

[23] T. Kapale and J. P. Dowling, Phys. Rev. Lett. **95**,173601 (2005);. Thanvanthri, K. T. Kapale and J. P. Dowling, Phys. Rev. A **77**, 053825 (2008).

[24] S. Thanvanthri, KT Kapale, JP Dowling, Journal of Modern Optics **59**,1180(2012)

[25] Z. F. Xu, P. Zhang, R. Lü and L. You, Phys. Rev. A **81**, 053619(2010)

[26] Y.-Z. Zhang, J. Luo, and Y.-X. Nie, Mod. Phys. Lett. A **16**, 789 (2001); C. Jacinto de Matos, J. Supercond. Nov. Magn. **24**, 193(2011).

[27] A. A. Svidzinsky and A. L. Fetter, Phys. Rev. Lett. **84**, 5919 (2000); A. L. Fetter, Rev. Mod. Phys. **81**, 647 (2009); P. Kuopanportti, E. Lundh, J. A. M. Huhtamäki,V. Pietilä, and M. Möttönen, Phys. Rev. A 81, 023603 (2010); P. Kuopanportti and M. Möttönen, *ibid*. **81**, 033627 (2010).

[28] E. C. Samson, K. E. Wilson, Z. L. Newman, and B. P. Anderson, Phys. Rev. A **93**, 023603 (2016).

[29] M. Quiroga-Teixeiro and H. Michinel, J. Opt. Soc. Am. B **14**, 2004 (1997); R. L. Pego and H. A. Warchall, J. Nonlin. Sci. **12**, 347 (2002); A. S. Reyna, G. Boudebs, B. A. Malomed, and C. B. de Araújo, Phys. Rev. A **93**, 013840 (2016).

[30] H. Sakaguchi, B. Li, and B. A. Malomed, Phys. Rev. E **89**, 032920 (2014); L. Salasnich, W. B. Cardoso, and B. A. Malomed, Phys. Rev. A **90**, 033629 (2014); H. Sakaguchi, E. Ya. Sherman, and B. A. Malomed, Phys. Rev. E **94**, 032202 (2016).

[31] Y.-C. Zhang, Z.-W. Zhou, B. A. Malomed, and H. Pu, Phys. Rev. Lett. **115**, 253902 (2015).

[32] F. Dalfovo and S. Stringari, Phys. Rev. A **53**, 2477 (1996) ; T. J. Alexander and L. Bergé, Phys. Rev. E **65**, 026611 (2002); L. D. Carr and C. W. Clark, Phys. Rev. Lett. **97**, 010403 (2006); D. Mihalache, D. Mazilu, B. A. Malomed, and F. Lederer, *ibid*. **73**, 043615 (2006).

[33] O. V. Borovkova, Y. V. Kartashov, L. Torner, and B. A. Malomed, Phys. Rev. E **84**, 035602 (R) (2011); R. Driben, Y. V. Kartashov, B. A. Malomed, T. Meier, and L. Torner, Phys. Rev. Lett. **112**, 020404 (2014).

[34] J. B. Sudharsan, R. Radha, H. Fabrelli, A. Gammal, and B. A. Malomed, Phys. Rev. A **92**, 053601 (2015).

[35] L. Bergé, Phys. Rep. **303**, 259 (1998); E. A. Kuznetsov and F. Dias, *ibid*. **507**, 43 (2011).

[36] C. Josserand, Chaos **14**, 875 (2004); J. K. Kim and A. L. Fetter, Phys. Rev. A **72**, 0236197 (2005); P. Kuopanportti and M. Mottonen, J. Low Temp. Phys. **161**, 561 (2010); D.-S. Wang, S.-W. Song, B. Xiong, and W.-Mi. Liu, Phys. Rev. A **84**, 053607 (2011); Y. Zhao, J. An, and C.-D. Gong, *ibid*. **87**, 013605 (2013); P. Kuopanportti, N. V. Orlova, and M. V. Milošević, *ibid*. **91**, 043605 (2015).

[37] Inouye, S., M. R. Andrews, J. Stenger, H. J. Miesner, D. M. Stamper-Kurn, and W. Ketterle, Nature (London) **392**, 151 (1998); T. Kohler, K. Goral, and P. S. Julienne, Rev. Mod. Phys. **78**, 1311 (2006); C. C. Chin, R. Grimm, P. Julienne, and E. Tsienga, *ibid*. **82**, 1225 (2010).

[38] L. Radzihovsky and D. E. Sheehy, Rep. Prog. Phys. **73**, 076501 (2010); X.-W. Guan, M. T. Batchelor, and C. Lee, Rev. Mod. Phys. **85**, 1633 (2013).

[39] B. D. Esry, C. H. Greene, J. P. Burke, and J. L. Bohn, Phys. Rev. Lett. **78**, 3594 (1997); M. L. Chiofalo, S. Succi, and M. P. Tosi, Phys. Rev. E **62**, 7438 (2000); W. Bao and Q. Du, SIAM J. Sci. Comput. **25**, 1674-1697 (2004).

[40] V. I. Kruglov, Yu. A. Logvin, and V. M. Volkov, J. Mod. Opt. **39**, 2277 (1992).

[41] R. Y. Chiao, E. Garmire, and C. H. Townes, Phys. Rev. Lett. **13**, 479 (1964).

[42] F. Maucher, S. Skupin and W. Krolikowski, Nonlinearity **24**, 1987 (2011).

[43] D. E. Pelinovsky, Y. S. Kivshar, and V. V. Afanasjev, Physica D **116**, 121 (1998); Y. S. Kivshar, D. E. Pelinovsky, T. Cretegny, and M. Peyrard, Phys. Rev. Lett. **80**, 5032 (1998)

[44] E. V. Doktorov, Phys. Lett. A **374**, 247 (2009)

[45] F. Maucher, E. Siminos, W. Krolikowski and S. Skupin, New J. Phys. **15**, 083055 (2013)

[46] W. J. Firth and D. V. Skryabin, Phys. Rev. Lett. **79**, 2450 (1997).

[47] H. Saito and M. Ueda, Phys. Rev. Lett. **89**, 190402 (2002).

[48] R. Zeng and Y. Z. Zhang, Computer Phys. Commun. **180**, 854 (2009).

[49] R. M. Caplan, Q. E. Hoq, R. Carretero-González, and P. G. Kevrekidis, Opt. Commun. **282**, 1399 (2009); R. M. Caplan, R. Carretero-González, P. G. Kevrekidis, and B. A. Malomed, Mathematics and Computers in Simulation 82, 1150 (2012).

[50] Y. S. Kivshar and G. P. Agrawal, *Optical Solitons: From Fibers to Photonic Crystals* (Academic Press, San Diego, 2003).

[51] R. L. Pego and H. A. Warchall, J. Nonlinear Sci. **12**, 347 (2002); M. Brtka, A. Gammal, and B. A. Malomed, Phys. Rev. A **82**, 053610 (2010).